CONCEPTUAL DESIGN OF A 0.2 MW PULSED 140 GHZ GYROKLYSTRON AMPLIFIER AND STUDIES TOWARDS 1 MW OPERATION FOR ACCELERATOR APPLICATION

A. Malygin, L. Feuerstein, M. Fuchs, S. Illy, J. Jelonnek, M. Thumm, A.-S. Müller
Karlsruhe Institute of Technology, Karlsruhe, Germany

Abstract

We present the conceptual design of two pulsed 140 GHz gyroklystron amplifiers intended as RF power sources for millimeter-wave accelerator systems. The interaction circuit in each design adopts a two-cavity configuration comprising an input cavity, a drift section, and an output cavity. The electron beam is generated by a triode-type magnetron injection gun (MIG), providing operational flexibility and stable performance across a broad operating range. Two gyroklystron configurations targeting output powers of 0.2 MW and 1 MW are investigated. Design details of the MIG and the interaction structures for both gyroklystron versions are presented.

INTRODUCTION

Exploration of accelerator technologies in the millimeter-wave regime offers a promising route toward extremely high accelerating gradients [1]. Owing to the high shunt impedance and short filling times of mm-wave accelerating structures relative to conventional S- and C-band systems, accelerating gradients at the GV/m level become attainable. Consequently, mm-wave accelerator concepts are of strong interest for applications such as future linear colliders, charged-particle therapy, compact X-ray free-electron lasers (XFELs), and ultrafast electron diffraction (UED) [2-4]. High-power RF sources operating in the mm-wave frequency range are therefore of considerable interest for advanced accelerator applications. This paper presents the design and simulation of two pulsed 140 GHz gyroklystrons [5-8] with target output powers of 0.2 MW and 1 MW. The 0.2 MW version is designed to operate together with a downstream pulse compressor to achieve the peak RF power levels required for high-gradient accelerator systems. In contrast, the 1 MW gyroklystron is intended to power accelerating structures directly, eliminating the need for additional pulse compression. The following sections describe the design methodology, interaction structures, and simulation results for both gyroklystron configurations.

CONCEPTUAL DESING OF A 0.2 MW PULSED 140 GHZ GYROKLYSTRON

Figure 1 illustrates a potential configuration for the 0.2 MW pulsed 140 GHz gyroklystron system. In this scheme, the input RF signal is generated by a pulsed extended interaction klystron (EIK) driven by a solid-state power amplifier (SSPA). The output RF power from the gyroklystron is subsequently compressed using a pulse compressor before being coupled into an accelerating structure for high-gradient applications.

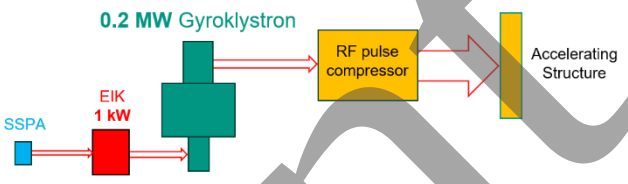

Figure 1: Layout of the 0.2 MW gyroklystron system including the SSPA, 1 kW EIK, and downstream RF pulse compressor.

The operating mode $TE_{7,3}$ in the output cavity was selected to minimize ohmic losses while providing sufficient beam–wave interaction to achieve 200 kW of output power. Simultaneously, the guiding center radius was chosen to be large enough to accommodate a 10 A electron beam while maintaining the required magnetic compression, emitter current density and guiding center spread. The design utilizes the following beam parameters: beam voltage $U = 60$ kV, beam current $I = 10$ A, pitch factor = 1.3, and a guiding center radius of 2.55 mm. A triode magnetron injection gun configuration (Fig. 2) was selected to provide enhanced flexibility in adjusting the electron beam parameters.

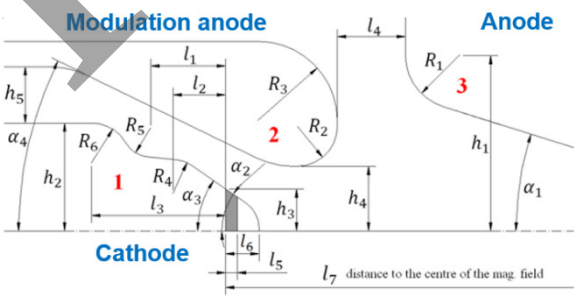

Figure 2: Configuration of the triode magnetron injection gun (MIG) with the key optimization parameters indicated.

The achieved electron beam parameters are summarized in Table 1; all values meet the specified requirements. The electron beam trajectories and the electric field distribution within the triode MIG are displayed in the top and bottom panels of Fig. 3, respectively. The two-cavity configuration, shown in Fig. 4, consists of an input cavity, a drift section, and an output section. Multimode simulations were performed using simpleRICK [5], an in-house code developed at the Institute for Pulsed Power and Microwave Technology (IHM) at the Karlsruhe Institute of Technology (KIT).

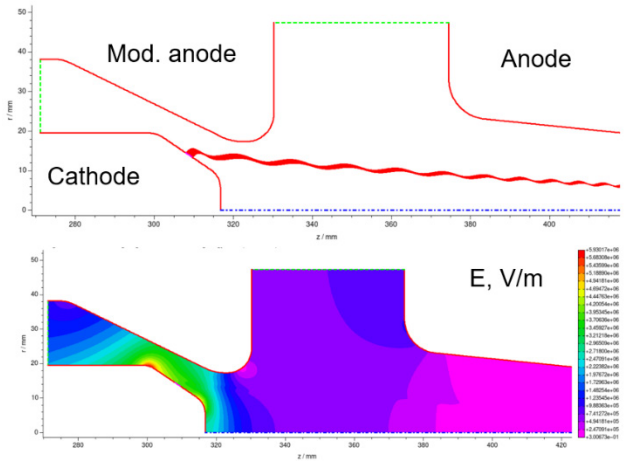

Figure 3: Triode magnetron injection gun showing electron trajectories (top) and the applied electric field distribution (bottom).

Table 1: Triode Magnetron Injection Gun Parameters

Parameters	Design values (requirements)	Simulation results
Pitch factor α	1.3 – 1.5	1.3 – 1.5
α spread, %	< 10	9
Guiding centre radius, mm	2.55	2.56
Guiding centre radius spread, mm	< 0.43 (λ/5)	0.4
Surface electric field, MV/m	< 6	5.9
Emitter current density, A/cm^2	< 4	2.6
Magnetic compression	< 45	29.5

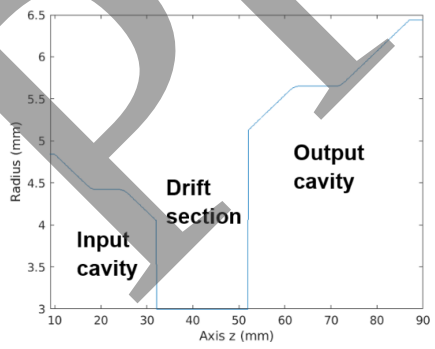

Figure 4: Configuration of the two-cavity interaction region, showing the input cavity, drift section, and output cavity.

The field distributions for the operating modes $TE_{7,2}$ in the input cavity and $TE_{7,3}$ in the output cavity are shown in Fig. 5. Figure 6 displays the spectra for these modes, demonstrating successful amplification and the suppression of competing modes. An output power of 250 kW was achieved. Ohmic cavity loss densities were estimated using the EURIDICE [6] code and are approximately 4 kW/cm² at the 250 kW-power level.

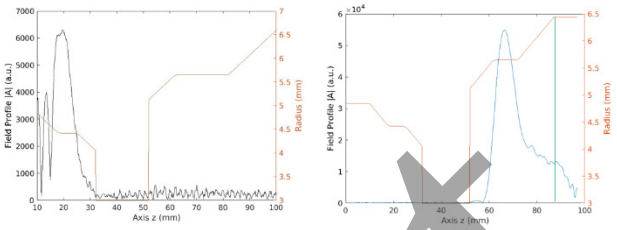

Figure 5: Field distributions of the $TE_{7,2}$ mode in the input cavity (left) and the $TE_{7,3}$ mode in the output cavity (right).

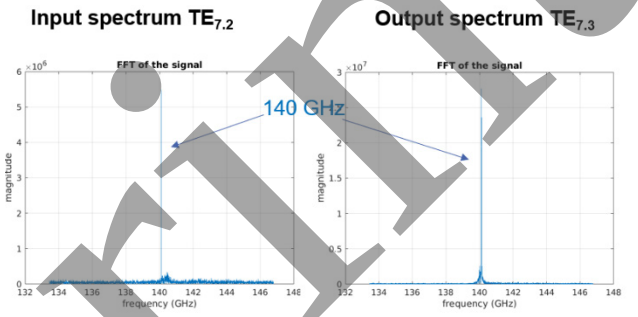

Figure 6: Spectra of the input cavity mode $TE_{7,2}$ (left) and the output cavity mode $TE_{7,3}$ (right).

STUDIES TOWARDS 1 MW 140 GHZ PULSED GYROKLYSTRON

A potential operating scheme for a 1 MW pulsed gyroklystron is shown in Fig. 7. As described further in this paper, the 1 MW unit requires a 10 kW gyroklystron pre-amplifier, the design of which is currently in progress. This preamplifier can utilize a commercially available solid-state power amplifier (SSPA) as its input signal source. This configuration eliminates the need for a pulse compressor by replacing the 1 kW extended interaction klystron (EIK) with the more powerful 10 kW gyroklystron.

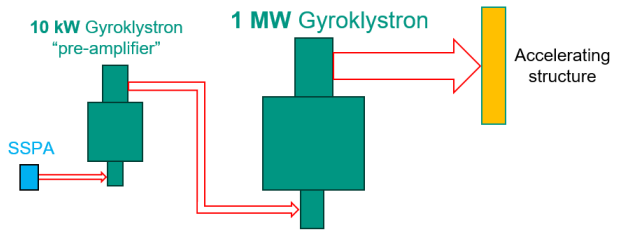

Figure 7: Schematic of the 1 MW gyroklystron system (without an RF pulse compressor), featuring an SSPA, a 10 kW gyroklystron preamplifier, and the 1 MW gyroklystron.

The cavity configuration is shown in Fig. 8. It utilizes a two-cavity design similar to the 0.2 MW gyroklystron previously discussed. However, due to the significantly increased RF and electron beam power, a higher-order mode and a larger guiding center radius are required. For a target output power of 1 MW at 30% efficiency, the

electron beam power must be approximately 3.2 MW, which can be achieved with a beam voltage of 80 kV and a current of 40 A. Preliminary estimations for the triode gun configuration indicate that to satisfy the beam parameters listed in Table 1, the guiding center radius must exceed 5 mm. Mode selection analysis shows that the $TE_{16,2}$ mode meets these requirements. Its closest competitor with a similar coupling coefficient is nearly 7 GHz away; all other competing modes have coupling coefficients at least 30% to 50% lower than the $TE_{16,2}$ mode. The $TE_{16,2}$ cavity has a radius of 7.92 mm and a guiding center radius of 5.82 mm. These parameters enable a 40 A current with a magnetic compression of 35, a guiding center radius spread of 0.42 mm, and an emitter current density of 3.7 A/cm^2, all of which are within requirements. Multimode simulations performed with the simpleRICK code accounted for 17 competing modes: $TE_{15,2}$, $TE_{20,1}$, $TE_{-4,6}$, $TE_{-9,4}$, $TE_{-12,3}$, $TE_{-2,7}$, $TE_{0,7}$, $TE_{21,1}$, $TE_{-7,5}$, $TE_{-10,4}$, $TE_{5,6}$, $TE_{-13,3}$, $TE_{3,7}$, $TE_{22,1}$, $TE_{1,8}$, and $TE_{17,2}$. The resulting field distribution for the $TE_{16,2}$ mode in the input cavity is shown in Fig. 8.

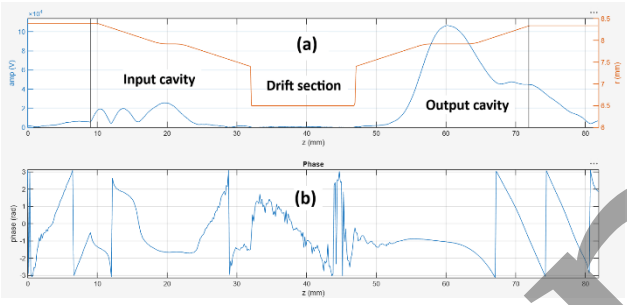

Figure 8: Field distribution of main mode $TE_{16,2}$ in the input and output cavity (a) and phase (b).

In order to increase the output power and identify a stable amplification regime, several parameters were optimized, including the lengths of the input, drift, and output sections, as well as the input power. Each configuration was used to scan the magnetic field from 5.55 T to 5.65 T. Figure 9 illustrates this magnetic field scan, followed by a period of constant magnetic field after 220 ns to verify mode stability. As shown, an output power of 800 kW was achieved with an input power of 9 kW at a frequency of 140.8 GHz, corresponding to an efficiency of 25% and a gain of 19.5 dB. Estimations of the Ohmic losses were performed using the EURIDICE code, resulting in approximately 8.9 kW/cm^2 at 800 kW and 3 kW/cm^2 at 270 kW for potential CW operation.

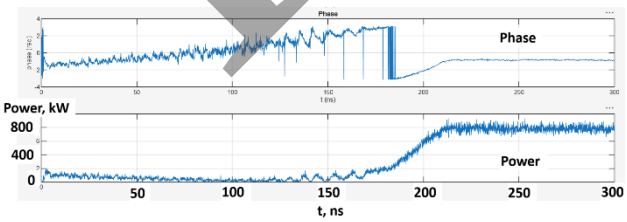

Figure 9: Output power of the $TE_{16,2}$ mode (bottom) and its corresponding phase (top).

The spectra of the input and output cavity mode $TE_{16,2}$ shown in Fig. 10 demonstrate successful amplification at the input frequency.

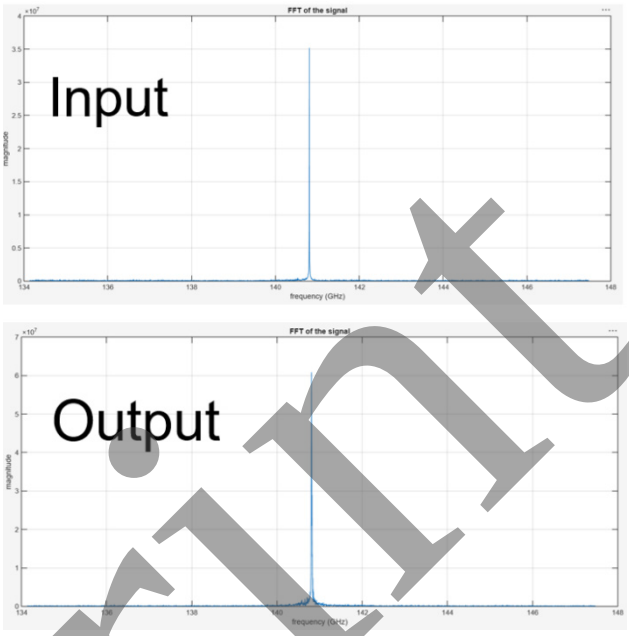

Figure 10: Spectra of the input cavity mode $TE_{16,2}$ (top) and the output cavity mode $TE_{16,2}$ (bottom).

CONCLUSION

This paper presented the conceptual designs of two 140 GHz pulsed gyroklystrons. For the 0.2 MW version, optimization of the magnetron injection gun and interaction region enabled the achievement of the required electron beam parameters and an output power of 250 kW for 1 kW of input power. This design utilizes the $TE_{7,2}$ and $TE_{7,3}$ modes in the input and output cavities, respectively.

Studies toward 1 MW operation indicate that the $TE_{16,2}$ mode allows for a magnetron injection gun design that satisfies the necessary beam parameters. Multimode non-stationary simulations with the simpleRICK code showed that stable single-mode amplification was achieved with this configuration, reaching an output power of 800 kW with 9 kW of input power. Further optimization of the magnetron injection gun and interaction region is ongoing to reach the target 1 MW output power level.

REFERENCES

[1] M. K. Othman *et al.*, "Experimental demonstration of externally driven millimeter-wave particle accelerator structure", *Applied Physics Letters*, vol. 117, 2020. doi:10.1063/5.0011397

[2] E. A. Nanni *et al.*, "Terahertz-driven linear electron acceleration", *Nature Commun.*, vol. 6, p. 8486, 2015. doi:10.1038/ncomms9486

[3] P. Salén *et al.*, "State-of-the-art electron beams for compact tools of ultrafast science", *Ultramicroscopy*, vol. 268, p. 114080, 2025. doi:10.1016/j.ultramic.2024.114080

[4] F. X. Kärtner, "Terahertz accelerator based electron and x-ray sources", *Terahertz Sci. Technol.*, vol. 13, no. 1, pp. 22–31, 2020.

[5] G. S. Nusinovich, M. K. A. Thumm, and M. I. Petelin, “The gyrotron at 50: Historical overview”, *J. Infrared Millim. Terahertz Waves*, vol. 35, no. 4, pp. 325–381, 2014. doi:10.1007/s10762-014-0050-7

[6] N. I. Zaitsev *et al*., “Pulsed high-order volume mode gyroklystron”, *Radiophys. Quantum Electron*., vol. 48, pp. 737–740, 2005. doi:10.1007/s11141-006-0002-8

[7] L. J. R. Nix *et al*., “Design and simulation of a high-power 48 GHz gyroklystron amplifier for accelerator applications”, in *Proc. IVEC’21*, Monterey, CA, USA, Apr. 2021, pp. 1–2. doi:10.1109/IVEC51707.2021.9722399

[8] A. V. Malygin *et al*., “Study of the scenario of switching-on of a pulsed gyrotron with a relativistic electron beam”, *Radiophys. Quantum Electron.*, vol. 53, no. 3, pp. 196–199, 2010.